Understanding the binding affinity of noscapines with protease of SARS-CoV-2 for COVID-19 using MD simulations at different temperatures

Durgesh Kumar, Kamlesh Kumari, Abhilash Jayaraj, Vinod Kumar, Ramappa Venkatesh Kumar, Sujata K. Dass, Ramesh Chandra & Prashant Singh

Check for updates

Understanding the binding affinity of noscapines with protease of SARS-CoV-2 for COVID-19 using MD simulations at different temperatures

Durgesh Kumar[a,b], Kamlesh Kumari[c], Abhilash Jayaraj[d], Vinod Kumar[e], Ramappa Venkatesh Kumar[f], Sujata K. Dass[g], Ramesh Chandra[b] and Prashant Singh[a]

[a]Department of Chemistry, A.R.S.D. College, University of Delhi, New Delhi, India; [b]Drug Discovery & Development Laboratory, Department of Chemistry, University of Delhi, Delhi, India; [c]Department of Zoology, D.D.U. College, University of Delhi, New Delhi, India; [d]SCFBio, Indian Institute of Technology, New Delhi, India ; [e]Special Centre for Nano Sciences, Jawaharlal Nehru University, Delhi, India; [f]Department of Zoology, Babasaheb Bhimrao Ambedkar University, Lucknow, UP, India; [g]Department of Neurology, BLK Super Speciality Hospital, New Delhi, India

Communicated by Ramaswamy H. Sarma

ABSTRACT

The current outbreak of a novel coronavirus, named as SARS-CoV-2 causing COVID-19 occurred in 2019, is in dire need of finding potential therapeutic agents. Recently, ongoing viral epidemic due to coronavirus (SARS-CoV-2) primarily affected mainland China that now threatened to spread to populations in most countries of the world. In spite of this, there is currently no antiviral drug/ vaccine available against coronavirus infection, COVID-19. In the present study, computer-aided drug design-based screening to find out promising inhibitors against the coronavirus (SARS-CoV-2) leads to infection, COVID-19. The lead therapeutic molecule was investigated through docking and molecular dynamics simulations. In this, binding affinity of noscapines(23B)-protease of SARS-CoV-2 complex was evaluated through MD simulations at different temperatures. Our research group has established that noscapine is a chemotherapeutic agent for the treatment of drug resistant cancers; however, noscapine was also being used as anti-malarial, anti-stroke and cough-suppressant. This study suggests for the first time that noscapine exerts its antiviral effects by inhibiting viral protein synthesis.
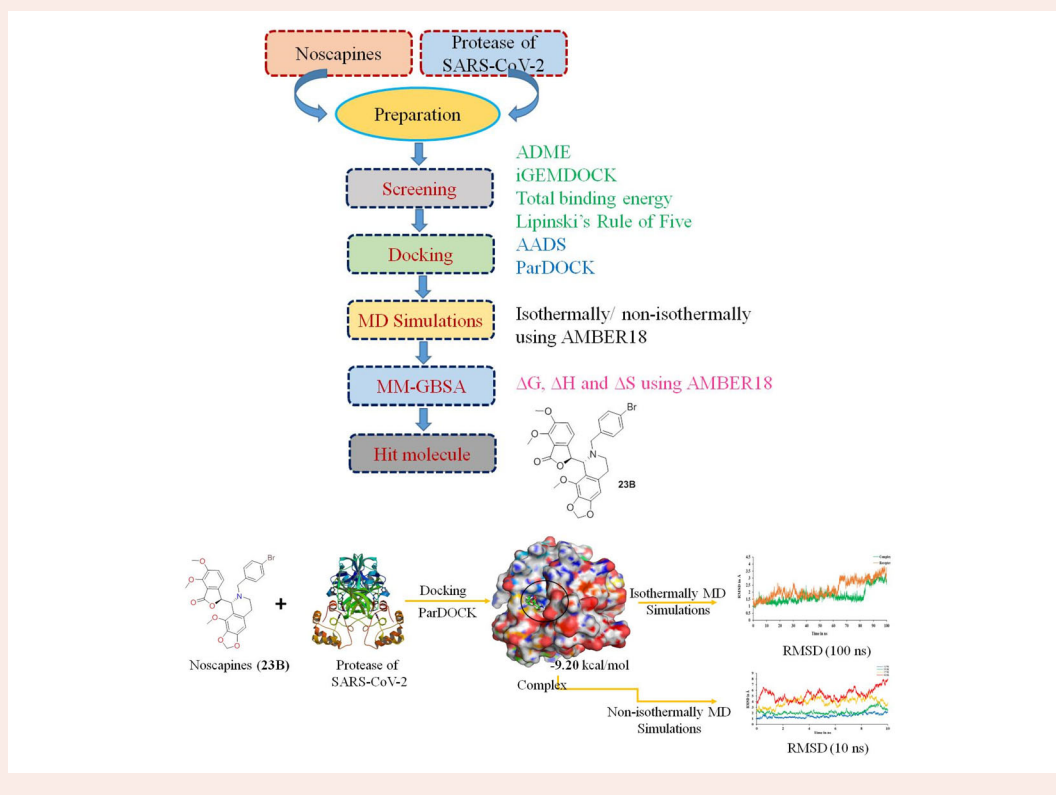
Introduction

Life may be a marvel and there's no unequivocal definition, but passing is cessation of all organic capacities that maintain a living being. Researchers have utilized physical sciences, counting quantum material science to clarify different marvels of life. The organic structures of a living being are subject to physical laws; for illustration, a life form is an open framework and must depend on its environment to a closed framework, and it takes after the moment law of thermodynamics by means of trade of data and mass and vitality. The infection called COVID-19, is caused by unused endemic crown infection (SARS-CoV-2), is odd – and appallingly particular. A later consider concluded that individuals with sort A blood gather may have a better chance of contracting this modern crown infection than individuals with sort O do. A few individuals tainted with the SARS-COV-2 infection feel alright, whereas others – indeed those who are sound and moderately youthful – get exceptionally ill. The COVID-19 widespread seem have tainted 90% of the world populace and slaughtered more than 40.6 million individuals in the event that no moderation measures were put in place to combat it by the individual states all inclusive (Agarwal et al., 2020; Ai et al., 2020; Arshad Ali et al., 2020). As labs closed down, universally a few thousand researchers are redeploying to battle crown infection. So distant 19,25,440 affirmed cases of COVID-19 have been confirmed universally with adding up to 1,19,718 passings, and in Italy more than 20,465 passings have been reported so far. In joined together United States of America, more than 5,87,155 cases tainted by COVID-19 have been affirmed, and number is still rising. As the COVID-19 flare-up quickly advances, inquire about work to create an immunization and to test antivirals and other therapeutics proceeds in parallel to other measures (Abbad et al., 2019; Ahmed et al., 2020; Boldog et al., 2020; De Salazar et al., 2020). At present, there are no effective drugs available for control of coronaviruses infection causes COVID-19. Currently, researchers are working for development of therapeutic drugs to treat infections from coronavirus and control death cases throughout the world. The three dimensional structure of the protease of SARS-CoV-2 for COVID-19 in complex with N3 (PDB ID: 6LU7) is available on RCSB protein databank (Alfaro et al., 2019; Burley et al., 2018; Daoui et al., 2019). Our research group has established that noscapine is a chemotherapeutic agent for the treatment of drug resistant cancers, however, noscapine was also being used as anti-malarial, anti-stroke and cough-suppressant.

This work aims to contribute for the development of drug against the protease of SARS-CoV-2 to decrease the infection of coronacirus i.e. COVID-19. The authors screened designed noscapine and its derivatives against the protease of SARS-CoV-2. In this, the target protease of SARS-CoV-2 for COVID-19 (PDB id - 6LU7) was used to consider in screening protocol (Al-Johani et al., 2017; Chandra et al., 2020; Duan & Zhu, 2020). Screening of designed library was done through iGEMDOCK and then screen the hit molecules based on bioactive score and 'Lipinski's Rule of Five' from the SwissADME and Molinspiration, web servers (Aaboud & ATLAS Collaboration, 2017; Hsu et al., 2011). Based on screening, top hit molecule was taken for molecular docking and MD Simulations. Through this, the binding affinity or change in binding free energy of newly formed drug–target complex was determined by simulations method and deviations measured on increasing temperature (Aaboud et al., 2018; Adasme-Carreno et al., 2014; Athir et al., 2019; Goodsell et al., 2020). Herein, MM-GBSA method was to calculate the change in enthalpy and the change in free energy for the formation of complex, number of hydrogen bonds (HBs) are determined to study the binding of the hit molecule with the protease of SARS-CoV-2 for COVID-19. A detailed study will provide an understanding to the design of antiviral molecules to inhibit protease of SARS-CoV-2 of COVID-19.

Experimental methods

Target and ligand preparations

The three dimensional structure for the protease of SARS-CoV-2 of COVID-19 (PDB ID: 6LU7) was retrieved from RCSB Protein Data Bank (http://www.rcsb.org/structure/6LU7). Some missing atom and water molecules were removed in protein chains using Chimera and Notepad^{++}. The library of designed molecules of noscapines (Table 1) was created using CS ChemDraw in cdx format and it was saved in .pdb format using Marvin Sketch.

However, the designed molecules were filtered against the protease of SARS-CoV-2 for COVID-19 based on total energy or binding energy (kcal/mol) of drug–target complex using iGEMDOCK (Kumar et al., 2019; Singh et al., 2019; Zhao et al., 2019). Authors, used iGEMDOCK to understand the binding of noscapine and its derivatives with the target to find hit candidation. The absorption (% ABS) was calculated using the Equation (1) proposed by Zhao et al. (2019).

$$\% \ \mathbf{ABS} = \mathbf{109} - [\mathbf{0.345} \times \mathbf{topological \ polar} \ \mathbf{surface \ area} \ (\mathbf{TPSA})] \tag{1}$$

The binding affinity of noscapine and its derivative with protease of SARS-CoV-2 of COVID-19 was obtained using ParDOCK, a web server (Gupta et al., 2007). ParDOCK is based on docking scoring function, calculates energy based on Equation (2).

$$\mathbf{E} = \sum \mathbf{Eel} + \mathbf{EvdW} + \mathbf{Ehpb} \tag{2}$$
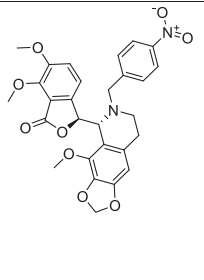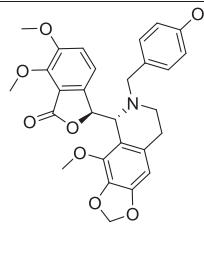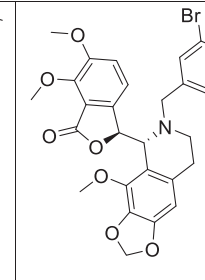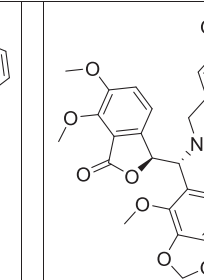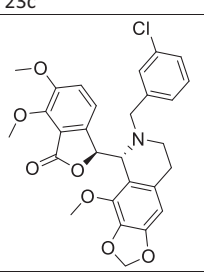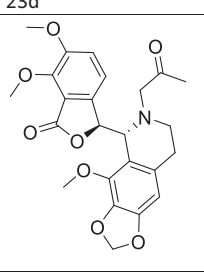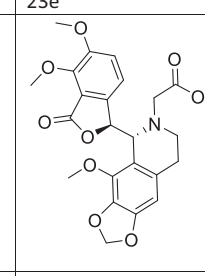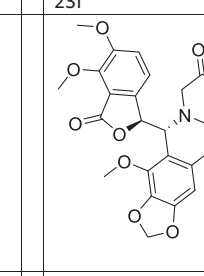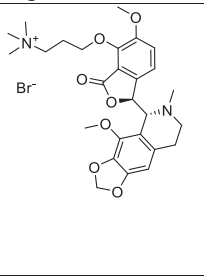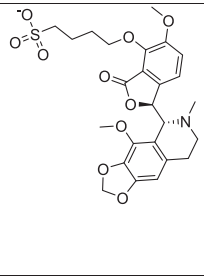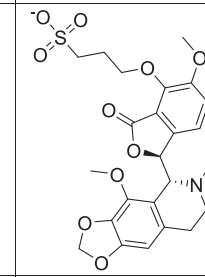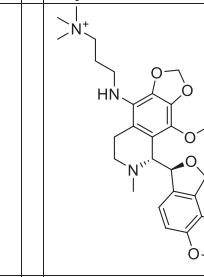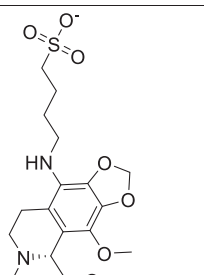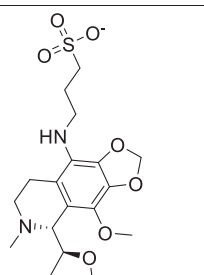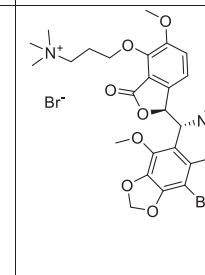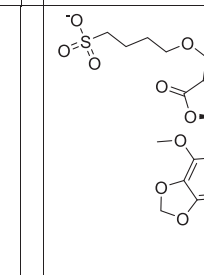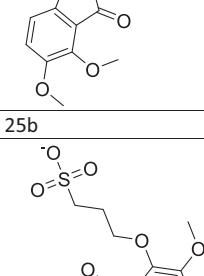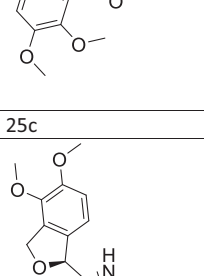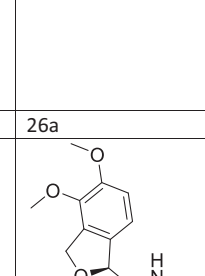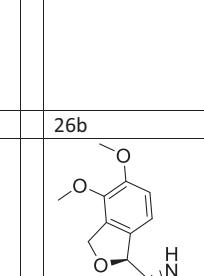
MD simulations of protease of SARS-CoV-2 of COVID-19 with and without screened ligand were performed using pmemd modules of AMBER, utilizing the ff14SB force field (Çınaroğlu & Timuçin, 2019; Skjevik et al., 2015). The three dimensional structure of noscapine and its derivatives were drawn using CS ChemDraw and Marvin sketch. Their optimization of the hit was done by Gaussian 09 (Ali et al., 2019; Chtita et al., 2019). Additionally, the parameters of noscapines for molecular dynamics simulation were generated using antechamber module of AMBER suite utilizing Generalized Amber Force Field (David et al., 2005; Roe & Cheatham, 2013, 2018; Vora et al., 2020). Different trajectories were drawn using the CPPTRAJ modules (David et al., 2005; Roe & Cheatham, 2013). The authors have analyzed the binding of screened noscapines with the protease of SARS-CoV-2 using trajectories to understand the stability and flexibility. The trajectories like root mean square deviation (RMSD), root mean square fluctuation (RMSF), HBs and change in binding free energy calculation will be

Table 1. List of designed noscapine and its derivatives.

13	14a	14b	14c
14d	15a	15b	15c
17	18	19	20
20a	20b	21a	21b
21c	21d	23a	23b
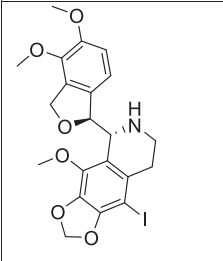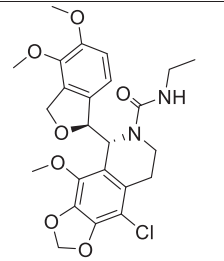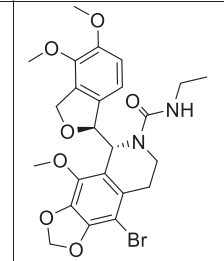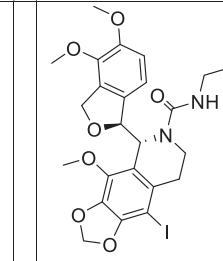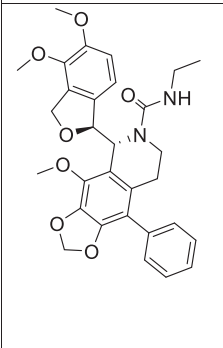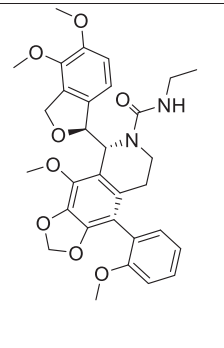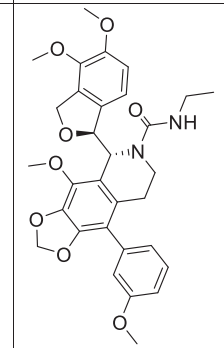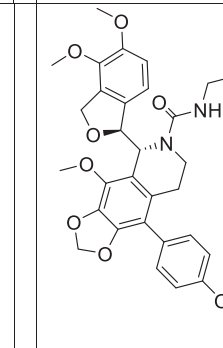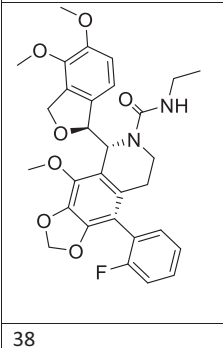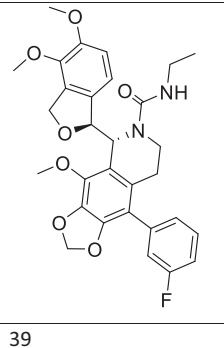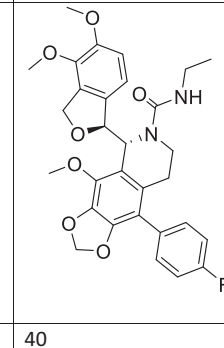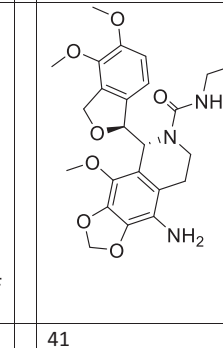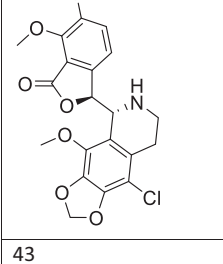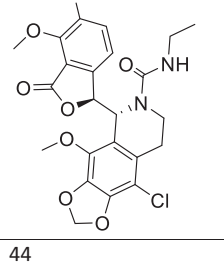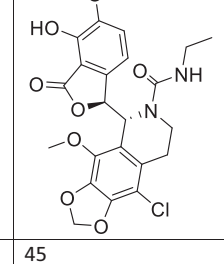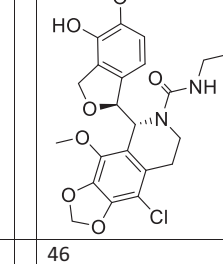
Table 1. Continued.

23c	23d	23e	23f
23g	23h	23i	23j
24a	24b	24c	25a
25b	25c	26a	26b
26c	27	28	29

Table 1. Continued.

30	31	32	33
34	35	36	37
38	39	40	41
43	44	45	46

determined by AMBER18 (Alexandrescu et al., 2001; David et al., 2005; Joshi et al., 2020).

RMSD plot is usually used to understand the stability of the complex as in Equation (3) while RMSF is used to understand the structural flexibility.

$$\text{RMSD} = \sqrt{\frac{1}{N}\sum_{i=1}^{N}\left(x_i^m - x_i^1\right)^2 + \left(y_i^m - y_i^1\right)^2 + \left(z_i^m - z_i^1\right)^2} \quad (3)$$

Where N is the number of atoms, x^m, y^m, z^m are the Cartesian coordinates of the initial structure and x^1, y^1, z^1 are the Cartesian coordinates of trajectory at frame t.

The RMSF equation is used to obtain the local structural flexibility and stability as in Equation (4) (Pant et al., 2017;

Pereira et al., 2019). These value are calculated based on equation given below.

$$\text{RMSF} = \sqrt{\frac{1}{T}\sum_{i=1}^{T}\left(X_i - \overline{X}\right)^2} \quad (4)$$

Where T is the number of trajectory frames and $\bar{x}$ is the time-averaged position.

Relative change in binding free energy calculations

Herein, MM-GBSA method is used to determine the change in enthalpy and change in free energy for the formation of complex, number of HBs to understand the binding of

screened noscapines with the protease of SARS-CoV-2 of COVID-19 (Al-Anazi et al., 2018; Chaudhari & Pahelkar, 2019; Chinnasamy et al., 2019; Du et al., 2011). It is considered to be more precise and the accurate to determine the relative change in free energies. From trajectories of MD productions, the relative change in enthalpy terms of complex, target protein, drug and difference in drug–target-complex at 100 and 10 ns are calculated by the given Equations (5)–(8) (Du et al., 2011; Gao et al., 2019; Hayes et al., 2011; Kalirajan et al., 2019).

$$\Delta G_{bind} = \Delta H - T\Delta S \tag{5}$$

$$\Delta H = \Delta E_{MM} + \Delta G_{solv} \tag{6}$$

$$\Delta E_{MM} = \Delta E_{internal} + \Delta E_{elec} + \Delta E_{vdw} \tag{7}$$

$$\Delta G_{solv} = \Delta G_{GB} + \Delta G_{SA} \tag{8}$$

Where, ΔE_{MM} is the change of the MM energy in the gas phase, which include $\Delta E_{internal}$, ΔE_{elec} is the electrostatic energy and ΔE_{vdw} is the van der Waals energy, ΔG_{solv} is the solvation free energy which is sum of electrostatic solvation energy, ΔG_{GB} is the polar contribution, calculated by solvent accessible surface area (SASA) and the nonelectrostatic solvation ΔG_{SA} is contributed by non-polar part.

Results and discussions

Noscapine is a heterocyclic compound and based on benzylisoquinoline. It is an alkaloid and known for its antitussive activity since last 90 years. It possesses various functional moieties. Noscapine is an anti-cancer molecule and the half-life of noscapine is 1.5 to 4 h. This molecule is a non-competitive antagonist of bradykinin receptors. It is used to protect some organs against ischemia–reperfusion injury (Kumar et al., 2019).

The designed library of noscapines was screened against the binding site of protease of coronavirus based on generic evolutionary method (GA). iGemdock give a molecule conformation and orientation relative to the active site of target protein and the GA parameters for screening: population size = 200, generations = 70, number of solution = 3. Based on screening results, it was found that noscapine (23B) effectively binds with COVID-19 and number of violations of Lipinski's Rule of Five is <1.[42] iGEMDOCK calculate the total binding energy of designed noscapine with protease of coronavirus and are summarized in Table 2.

The binding energy is due to the energy contributed by different amino-acids or residues around the cavity of target protein on interaction with the screened molecule. These residues contribute energy due to different interactions like hydrogen bonding, vdW, electrostatic interactions, π-π stacking, etc.

Thus, the interaction contribution for screened hit molecule (23B) was analyzed through post screening approach of iGEMDOCK. The $\delta G_{binding}$ versus interacted residues of the binding were plotted as in Figure 1. The complex of noscapine (23B) has shown minimum total binding energy of −118.652 kcal/mol. The major contributions of interacted residues with 23B are ARG40, TYR54, CYS85, PHE181, ARG188,

Table 2. Screening results of few prominent noscapine based on total energy against protease of coronavirus using iGEMDOCK tools.

Ligand	T. Energy	Ligand	T. Energy	Ligand	T. Energy	Ligand	T. Energy
23B	−118.652	15b	−108.526	15a	−102.645	30	−96.1478
25B	−115.479	27	−108.06	13	−102.328	23H	−95.6639
34	−114.496	26B	−107.919	24A	−102.041	15c	−94.9549
25C	−113.261	24B	−106.265	46	−101.243	45	−94.8904
44	−113.129	39	−106.183	25A	−100.895	21B	−93.845
43	−112.93	23F	−106.096	14b	−100.456	29	−93.4034
35	−112.841	36	−105.854	17	−100.34	33	−93.2549
38	−112.655	26C	−105.594	23A	−100.054	24C	−93.1958
23E	−111.351	32	−105.313	23G	−99.2819	14d	−92.3744
23D	−111.031	20	−105.083	18	−98.1615	28	−92.2761
20B	−109.709	23J	−103.999	31	−97.8445	21D	−92.1422
37	−109.637	20A	−103.833	14a	−97.49	14c	−91.7612
23I	−109.209	41	−103.3	26A	−96.9662	21A	−91.0008
40	−108.584	23C	−103.214	19	−96.3373	21C	−90.6609

ARG40, TYR54, GLU55, MET82 and ASN84. Three dimensional structure of 23B is shown in Figure 2.

From Lipinski's Rule of Five states that the noscapine (23B) showed good membrane permeability due to have LogP ≤ 5, molecular weight ≤ 500, the number of hydrogen bond acceptors ≤ 10, and the number of hydrogen bond donors ≤ 5 including % absorptions based on Equation (2). Further, the SwissADME Web tool was used to calculate physicochemical, pharmacokinetic, drug like and other related parameters for hit molecules as in Table 3. Moreover, for drug development targeting oral administration, the solubility is one of the key properties in the influencing of drug absorption (Kumar et al., 2019; Yuan et al., 2017). Thus, sparingly soluble drugs can deliver an enough quantity of active ingredient into target site in the pharmaceutical dosage. It was observed that the CMPD23B, the hit molecule follows all the parameters of drug likeness score with one violation. In the criteria of drug likeness, one or no violation is considered as a biological potent molecule.

In Figure 3, the pink area of hit molecule, CMPD23B represented the optimal range for different properties like lipophilicity (–0.7 to +5.0), size less than 500, polarity, TPSA (20 to 130 A^2), solubility <6 and flexibility <9. The area of the screened noscapine derivative is proven to be a useful descriptor in the drug development to quickly estimate some ADME properties.

Based on screening results, top hit molecule i.e CMPD23B from of designed library was used for molecular docking. In docking study, prepared target protein and drug molecule were loaded into ParDOCK, a web server. Thus, the selection of best conformations was done on the basis of interaction energy or binding affinity between two interacting system. Docking results theoretically proved interacted residue around drug molecules with their distance cutoff are HIE163-H = 4.50, HIE163-O = 3.01, HIE163-Ar = 6.05, SER147-H = 3.65, MET49-Ar = 7.79, GLY143-O = 3.65, ASN142-O = 4.47, ASN142-H = 3.39, HIE164-H = 4.23, HIE164-H = 6.20, SER144-H = 3.88, SER144-O = 4.03, HIE41-Ar = 7.83, MET165-Ar = 5.16, CYS145-O = 3.93 and CYS145-Ar = 3.91, respectively, as in Figure 4(a). After successful generation of docking, the docked poses were analysed into active site of target protein is mentioned in Figure 4(b). Docking results of the docked ligand (N3) available in the PDB: 6LU7 interacted with the residues with their distance cutoff are HIS163-H = 5.24, GLY143 = 3.56, HIS164 = 6.32, GLN189 = 4.69, GLU166 = 4.97,
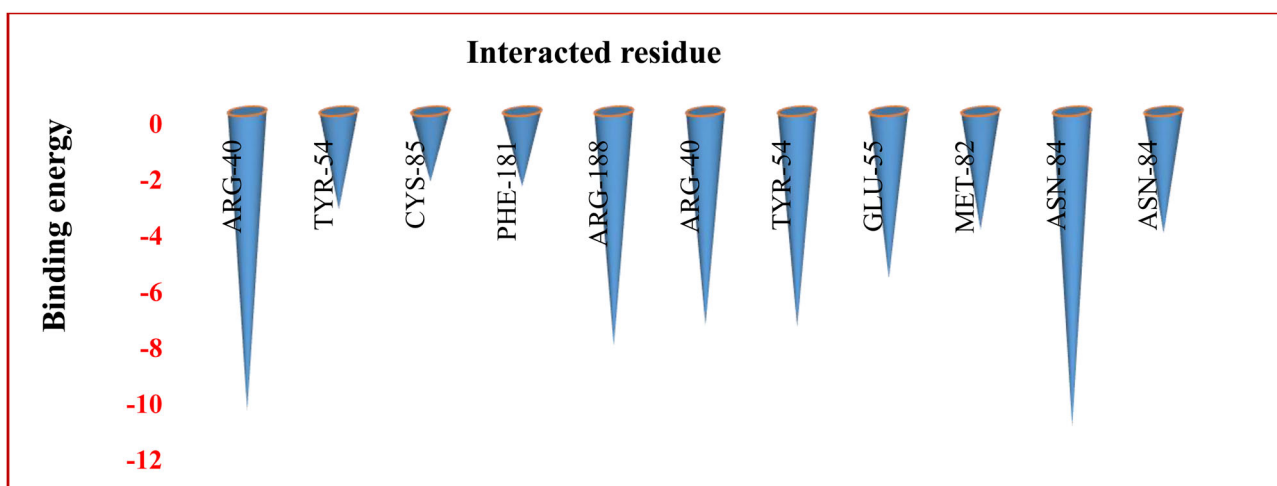
Figure 1. Interaction of the residues of protease of coronavirus for COVID-19 with CMPD23B.
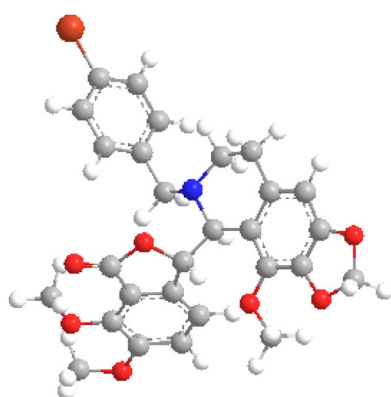

Figure 2. The 3D representations of top hit noscapines (CMPD23B).

Table 3. Physicochemical and bioactive parameters of screened hit (CMPD**23B**).

Properties	Noscapine (23B)
Log S (ESOL) mol/L	3.90×10^{-7}, poorly soluble
Heavy atoms	37
MW (g/mol)	568.41
No. of rotational bonds	6
No. H-bond acceptors	8
Num. H-bond donors	0
Log $P_{o/w}$(**iLOGP**)	4.29
GPCR ligand	−0.11
Lipinski's rule of five	Yes; 1 violation: MW > 500
Log K_p (skin permeation) cm/s	−6.30
TPSA(Å^2)	75.69
% ABS	82.88
Bioavailability score	0.55
Synthetic accessibility	4.71

Figure 3. Physiochemical space for oral bioavailability score enables a first glance at the drug-likeness of a molecule.

backbones participates in the hydrogen bonding (Agarwal et al., 2015; Alamri and Alamri, 2019; Ali & Shar, 2019; Scott & Ron, 2018). The hit molecule (CMPD23B) apart from forming the hydrogen bonds binds in the hydrogen accepter favorable, hydrogen donor favorable region, various stacking occurs in electrostatic favorable regions and van der Waals interactions in the region of steric favorable with protease of coronavirus as in Figure 5(a–d).

Isothermally MD simulations

The MD simulations of drug–target complex were effectively run for 100 ns time scale. In order to measured structural stability of the newly formed complex and difference of the stabilities in the protease of corona virus with and without molecule (Do et al., 2018). In MD simulations, authors have calculated the RMSD values of the backbone atoms relative to the complex structure through MD simulations as a function of time in Figure 6. It was seen that the complex of CMPD23B is stable til 83 ns time scale. For the complex system with 23B molecules, the average value of RMSD in ff14SB force field is 0.89 to 2.81 Å observed at 100 ns time scale. While the apo system without 23B molecules, the

PRO = 4.37, ALA191 = 5.31, LEU167 = 5.32, HIS172 = 5.49, respectively, as in Figure 4(c) and the docked pose is given in Figure 4(d).

In Figure 4(a), the dotted light green lines are showing hydrogen bond interaction with protease of coronavirus (SARS-CoV-2) while the other one does not. Apart from this, the residue HIE41 forms π-π T-shaped stacking with aromatic ring of molecule. Moreover, MET49 forms π-sulfur interaction and MET165 also forms a π-alkyl interaction with aromatic ring of the molecules. Other interactions are marked with blue dotted lines in the form of van der Waals interactions and π-donor hydrogen bonds. Here, three residues of
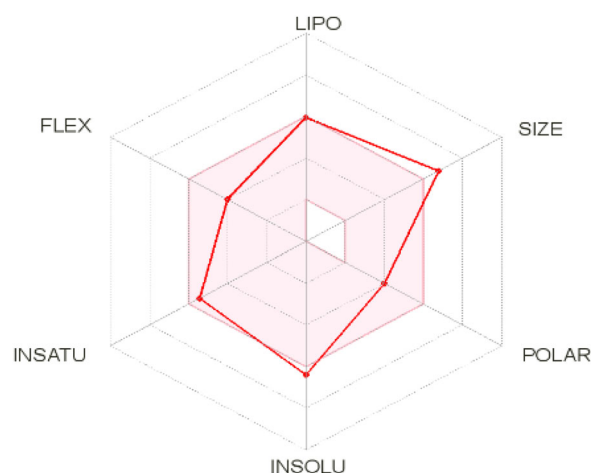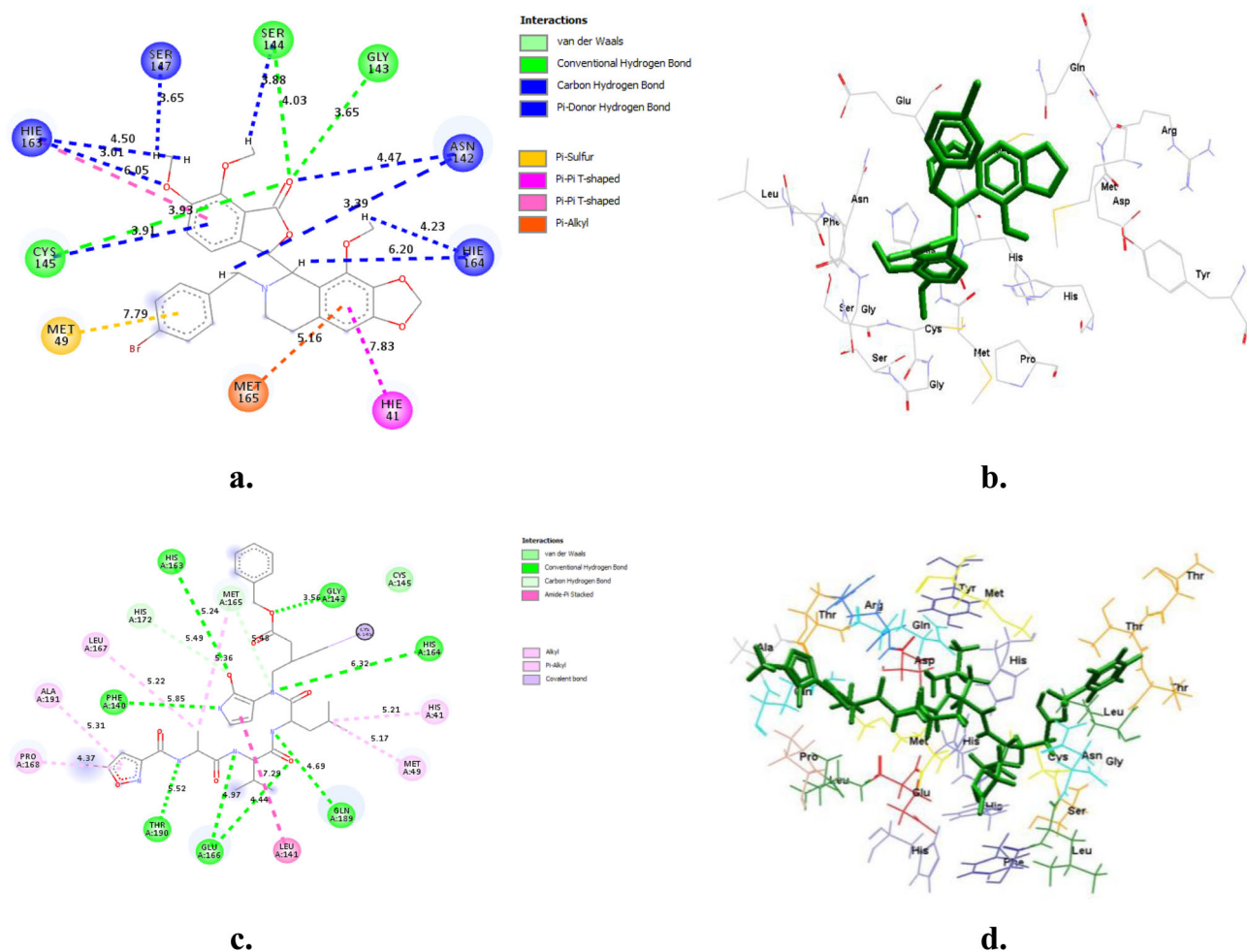
Figure 4. (a) & (c) shows the interaction of top hit molecule (23B) and N3 with protease of coronavirus for COVID-19 and (b) & (d) are Docked pose of hit molecule (23B) and N3 into the defined cavity.

RMSD value with same field is 0.86 to 3.87 observed at 100 ns scale. This showed that the trajectories of the MD simulations for the drug–target complex were more stable before 83 ns, so it was to do the HBs calculation and free energy decomposition based on the snapshots extracted for 100 ns.

Further, the detailed analysis of newly formed drug–target complex through root-mean-square fluctuation (RMSF) versus the residue number of protease of coronavirus for COVID-19 for top hit molecule is represented in Figure 7. It was observed that the complex of protease of coronavirus with 23B possess less fluctuations and indicates the interaction mode of the 23B with residues of protease of coronavirus for COVID-19. Moreover, the residues of binding site regions are HIE163, SER147, MET49, GLY143, ASN142, HIE164, SER144, HIE41, MET165 and CYS145 had showed a rigid behaviour with hit molecules. In short analysis, the RMSF plot indicates structural stability drug–target complex system is more stable under the influence of ff14SB force field than native protease of coronavirus for COVID-19.

RMSD plot can be used to understand the deviations between the crystal structure of protease of coronavirus of COVID-19 and the 23B-protease of coronavirus complex for 100 ns time scale. In Figure 6, the complex system before

83 ns showed minimum deviations and will be more structural stable. These results basically agree with the RMSD and RMSF analyses, it is used to determine the number of hydrogen bonds, enthalpy of complex system and decomposition of free energy .

MM-GBSA methods

In order to further explore the docking results, MD simulations at 100 ns for the complex between the protease of coronavirus for COVID-19 and CMPD23B were performed and the results were performed using different trajectories like number of hydrogen bonds, distance and angle of hydrogen as in Figure 8. The total numbers of average hydrogen bonds in MD simulations are calculated. Herein, two hydrogen bonds are formed in the complex in MD simulation. The average number of HBs of 23B at per residue different donor–acceptor average distance cutoffs is 2.86 (strong bonding) with larger average angle 159.68°. Change in enthalpy for the complex of protease of COVID-19 and 23B for MD simulation of 100 ns was determined and the plot is given in Figure 9. Change in enthalpy was found to be −35.65 kcal/mol as given in Table 4.
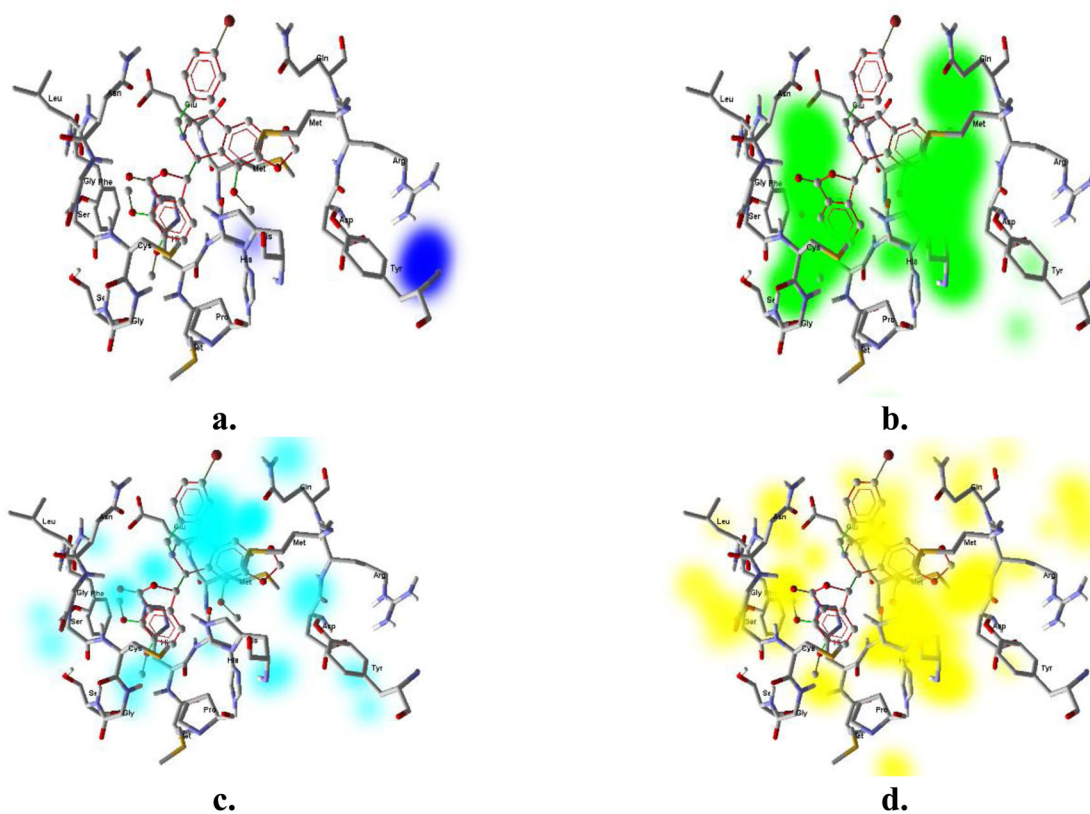
Figure 5. Various molecular interactions between CMPD23B and protease of SARS-CoV-2 are observed in different favorable regions (a) Electrostatic favorable; (b) Steric favorable; (c) Hydrogen accepter favorable; and (d) Hydrogen donor favorable.
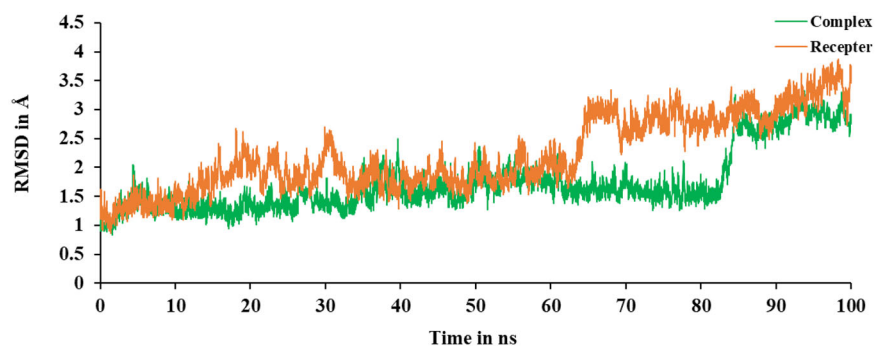
Figure 6. RMSD plot of protease of coronavirus for COVID-19 with and without CMPD**23B** as a function of time.
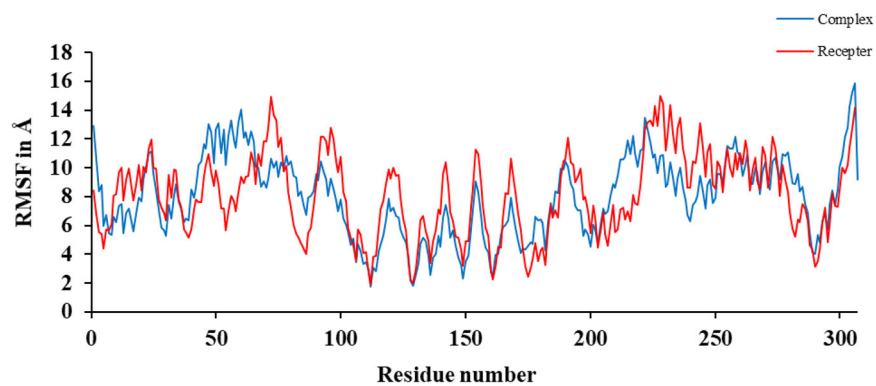
Figure 7. RMSF plot of protease of coronavirus for COVID-19 with and without CMPD**23B** at 100 ns time scale.
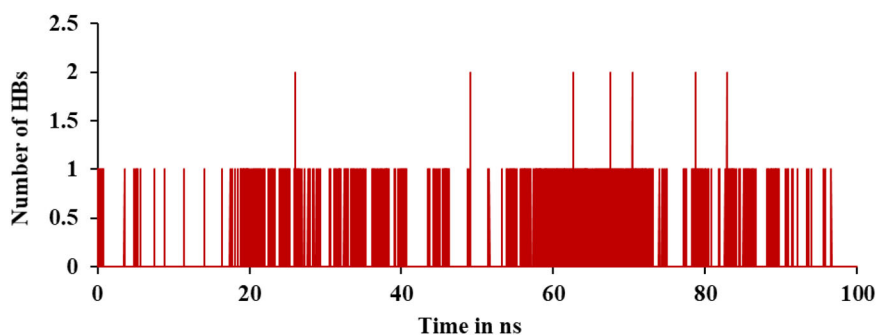
Figure 8. Number of hydrogen bonds of the complex of protease of coronavirus for COVID-19 with **23B** as a function of time are retained or broken during simulation time scale 100 ns.
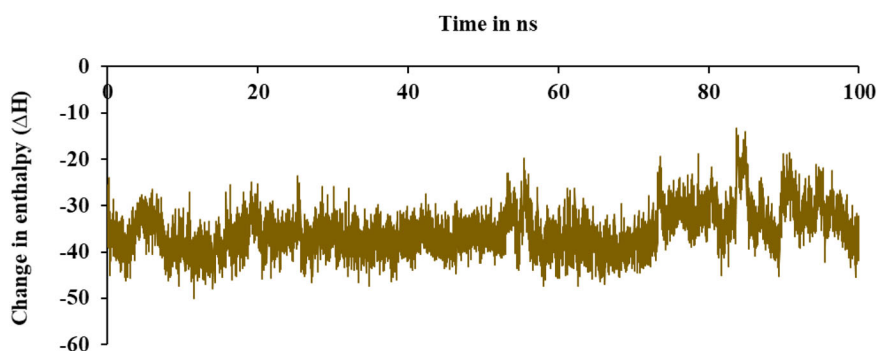
Figure 9. Enthalpy of the complex of protease of coronavirus for COVID-19 with 23B for MD simulation of 100 ns.

Table 4. Enthalpy for the formation of complex of protease of coronavirus for COVID-19 with 23B from MD simulation for 100 ns. [d- CMPD23; t-protease of coronavirus for COVID-19]

Energy Component	Complex (dt) Average	Receptor (t) Average	Drug (d, 23B) Average	d-t-dt complex (kcal/mol) Average
VDWAALS	−2437.68	−2381.69	−8.13	−47.85
EEL	−21,507.44	−21,475.56	−22.77	−9.11
ΔEGB	−3020.72	−3019.65	−27.30	26.23
ESURF	105.42	106.24	4.11	−4.93
ΔG_{gas}	−23,945.12	−23,857.26	−30.90	−56.96
ΔG_{solv}	−2915.29	−2913.41	−23.18	21.30
ΔH_{total}	−26,860.42	−26,770.67	−54.09	−35.65
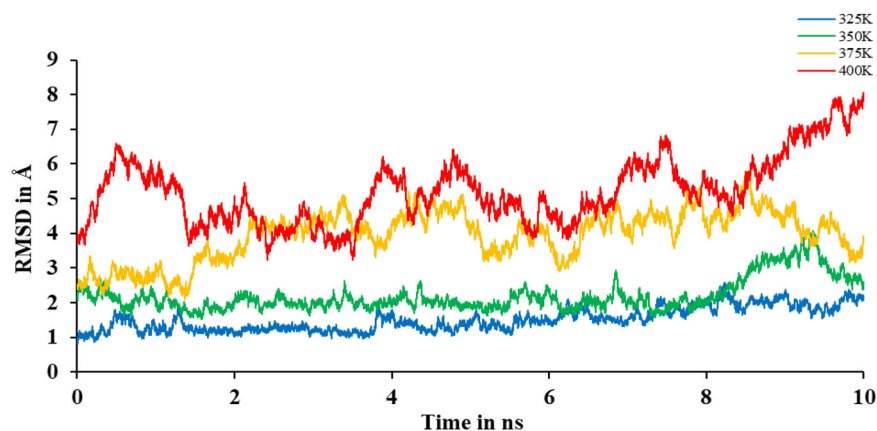
Figure 10. Non-isothermally RMSD plot for complex of protease of coronavirus for COVID-19 with 23B for MD simulations at 10 ns.

Non-isothermally MD simulations

There is a need to understand the binding of the screened noscapine derivative, i.e., 23B with protease of SARS-CoV-2 for COVID-19 at different temperatures and it was done by performing the MD simulations at 10 ns. The temperature for the MD simulations was increased to 400 K from 300 K with
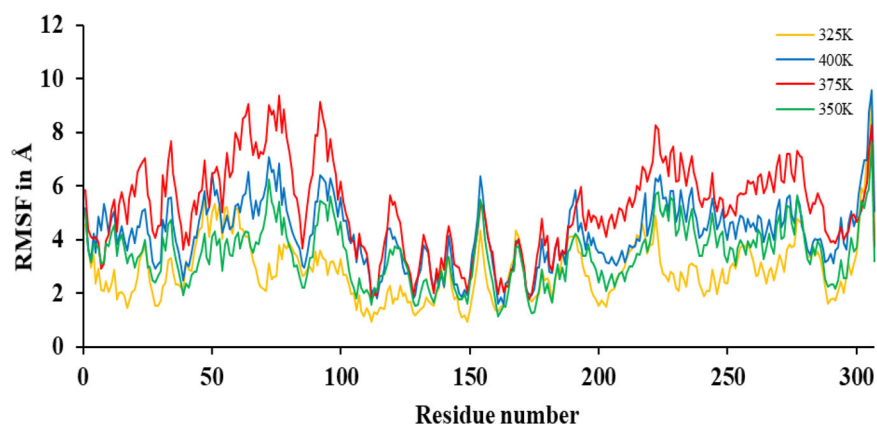
Figure 11. Non-isothermally RMSF plot for complex of protease of coronavirus for COVID-19 with 23B for MD simulations at 10 ns.

Figure 12. Number of HBs at 325 K for complex of protease of coronavirus for COVID-19 with 23B for MD simulations at 10 ns.

Figure 13. Number of HBs at 350 K for complex of protease of coronavirus for COVID-19 with 23B for MD simulations at 10 ns.

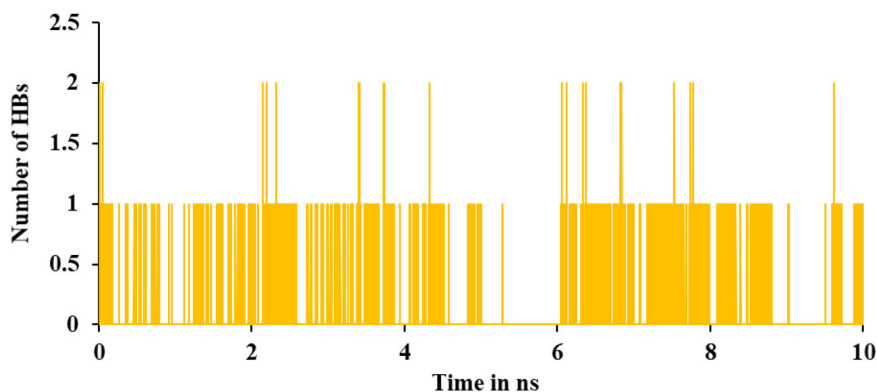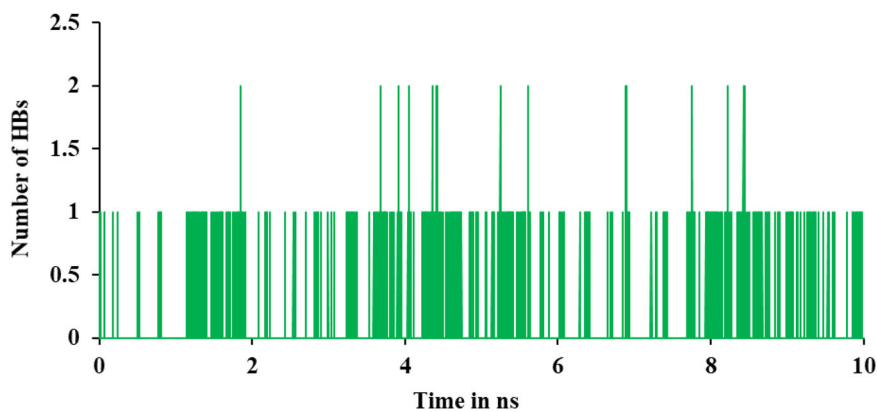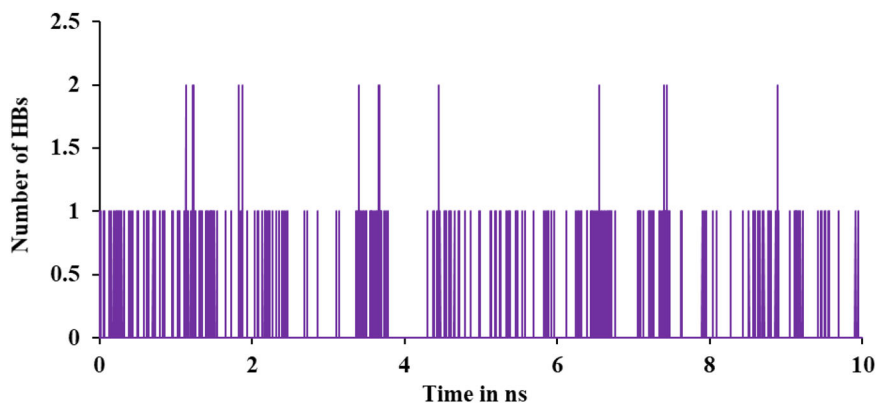**Figure 14.** Number of HBs at 375 K for complex of protease of coronavirus for COVID-19 with 23B for MD simulations at 10 ns.
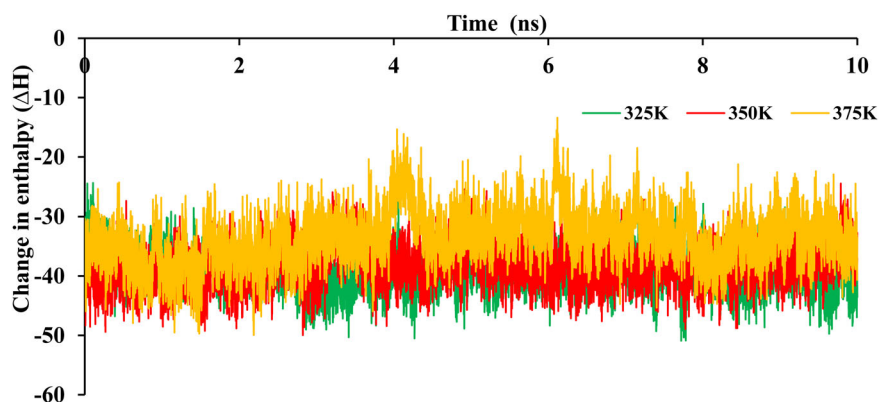
Figure 15. Enthalpy of the complex of protease of coronavirus of COVID-19 and 23B at different temperature for MD simulation of 10 ns.

Table 5. Thermodyanamic parameters for the formation of complex at different temperature.

Energy component	At 325 K	At 350 K	At 375 K
ΔH (kcal/mol)	−39.2085	−38.3836	−33.7549
$-T\Delta S$ (kcal/mol)	−32.0505	−31.3690	−33.2348
ΔG (kcal/mol)	−7.1580	−7.0147	−0.5201

an interval of 25 K. Different trajectories were drawn to study the impact of temperature (Wang et al., 2019). RMSD can be used to understand the stability of the complex formed between the protease of coronavirus for COVID-19 and 23B. Various thermodynamic parameters were calculated at different temperatures with filtration. Through Figure 10, it can be easily understand that the fluctuation is very large at 400 K as well go above 8 Ð, therefore, it is unacceptable. So, the theremodynamic parameters at 400 K are not calculated.

RMSF trajectories provide lots of information regarding the stability of the complex. High fluctuations in the plot indicate more flexibility as well the more of unstable bonds. On other side, low value or less fluctuation indicate well-structured regions in the complex means less distortion. RMSF plot indicate that minimum fluctuation or less distortion in protease of coronavirus is observed on binding with 23B as in Figure 11.

Hydrogen bonding during the formation of the complex between the protease of coronavirus and 23B play an important role in the binding as well as stability. Detailed analysis of the hydrogen bonds between drug and target protein are predicted under the influence of AMBER force field. Numbers of hydrogen bonds formed are 2 in each case, i.e., at different temperature between the protease of coronavirus for COVID-19 and 23B as Figures 12–14.

Different thermodynamic parameters like change in enthalpy, change in free energy for the complex of protease of coronavirus of COVID-19 and 23B for MD simulation of 10 ns were determined and the plot is given in Figure 15 and details is given in Table 5.

Based on Table 5, it can be understand that ΔH and ΔG are favorable for the formation of complex at 235 K.

Conclusion

Based on the results mentioned above, it can easily understand that the noscapine derivative, 23B has the ability to bind with the protease of coronavirus of COVID-19 effectively at 300 K. Further, the binding of 23B was studied at different temperature and found that the binding is best at 325 K. 23B has the potential to inhibit the protease of coronavirus of COVID-19 and effectively at 325 K. It has the possible to act as antiviral agent.

References

Aaboud, M., & ATLAS Collaboration. (2017). Determination of the strong coupling constant alpha s from transverse energy-energy correlations in multijet events at s = 8 TeV using the ATLAS detector. *The European Physical Journal C*, *77*(12), 872, 1-34. https://doi.org/10.1140/epjc/s10052-017-5442-0.

Aaboud, M., ATLAS Collaboration, Aad, G., Abbott, B., Abdinov, O., Abeloos, B., Abhayasinghe, D. K., Abidi, S. H., AbouZeid, O. S., Abraham, N. L., Abramowicz, H., Abreu, H., Abulaiti, Y., Acharya, B. S., Adachi, S., Adamczyk, L., Adelman, J., Adersberger, M., Adiguzel, A., … Zwalinski, L. (2018). Probing the quantum interference between Singly and Doubly resonant top-quark production in pp collisions at sqrt[s] = 13 TeV with the ATLAS Detector. *Physical Review Letters*, *121*(15), 152002.

Abbad, A., Perera, R. A., Anga, L., Faouzi, A., Minh, N. N. T., Malik, S. M. M. R., Iounes, N., Maaroufi, A., Van Kerkhove, M. D., Peiris, M., & Nourlil, J. (2019). Middle East respiratory syndrome coronavirus (MERS-CoV) neutralising antibodies in a high-risk human population, Morocco, November 2017 to January 2018. *Eurosurveillance*, *24*(48), 1900244. https://doi.org/10.2807/1560-7917.ES.2019.24.48.1900244

Adasme-Carreno, F., Munoz-Gutierrez, C., Caballero, J., & Alzate-Morales, J. H. (2014). Performance of the MM/GBSA scoring using a binding site hydrogen bond network-based frame selection: The protein kinase case. *Physical Chemistry Chemical Physics*, 16(27), 14047–14055. https://doi.org/10.1039/C4CP01378F

Agarwal, A., Nagi, N., Chatterjee, P., Sarkar, S., Mourya, D., Sahay, R. R., & Bhatia, R. (2020). Guidance for building a dedicated health facility to contain the spread of the 2019 novel coronavirus outbreak. *Indian Journal of Medical Research*. https://doi.org/10.4103/ijmr.IJMR_518_20

Agarwal, T., Asthana, S., & Bissoyi, A. (2015). Molecular modeling and docking study to elucidate novel chikungunya virus nsP2 protease inhibitors. *Indian Journal of Pharmaceutical Sciences*, 77(4), 453–460. https://doi.org/10.4103/0250-474X.164769

Ahmed, S. F., Quadeer, A. A., & McKay, M. R. (2020). Preliminary Identification of Potential Vaccine Targets for the COVID-19 Coronavirus (SARS-CoV-2) Based on SARS-CoV Immunological Studies. *Viruses*, 12(3), 254. https://doi.org/10.3390/v12030254

Ai, T., Yang, Z., Hou, H., Zhan, C., Chen, C., Lv, W., Tao, Q., Sun, Z., & Xia, L. (2020). Correlation of chest CT and RT-PCR testing in coronavirus disease 2019 (COVID-19) in China: A report of 1014 cases. *Radiology*. https://doi.org/10.1148/radiol.2020200642

Al-Anazi, M., Al-Najjar, B. O., & Khairuddean, M. (2018). Structure-based drug design studies toward the discovery of novel chalcone derivatives as potential epidermal growth factor receptor (EGFR) inhibitors. *Molecules*, 23(12), 3203. https://doi.org/10.3390/molecules23123203

Al-Johani, M. A., Al-Zaydi, K. M., Mousally, S. M., Alqahtani, N. F., Elnagdi, N. H., & Elnagdi, M. H. (2017). Multi component reactions under increased pressure: On the mechanism of formation of pyridazino[5,4,3-de][1,6]naphthyridine derivatives by the reaction of malononitrile, aldehydes and 2-oxoglyoxalarylhydrazones in Q-tubes. *Molecules*, 22(12), 2114. https://doi.org/10.3390/molecules22122114

Alamri, M. A., & Alamri, M. A. (2019). Pharmacophore and docking-based sequential virtual screening for the identification of novel Sigma 1 receptor ligands. *Bioinformation*, 15(8), 586–595. https://doi.org/10.6026/97320630015586

Alexandrescu, A. T., Snyder, D. R., & Abildgaard, F. (2001). NMR of hydrogen bonding in cold-shock protein A and an analysis of the influence of crystallographic resolution on comparisons of hydrogen bond lengths. *Protein Science*, 10(9), 1856–1868. https://doi.org/10.1110/ps.14301

Alfaro, S., Navarro-Retamal, C., & Caballero, J. (2019). Transforming non-selective angiotensin-converting enzymes inhibitors in C- and N-domain selective inhibitors by using computational tools. *Mini Reviews in Medicinal Chemistry*. https://doi.org/10.2174/1389557520666191224113830

Ali, L., Khan, S. U., Golilarz, N. A., Yakubu, I., Qasim, I., Noor, A., & Nour, R. (2019). A feature-driven decision support system for heart failure prediction based on chi (2) statistical model and Gaussian Naive Bayes. *Computational and Mathematical Methods in Medicine*, 2019, 1–8. https://doi.org/10.1155/2019/6314328

Ali, W., & Shar, N. A. (2019). Molecular docking analysis of timepidium with Acetylcholine and lumacaftor with GABA(A) activator. *Bioinformation*, 15(11), 832–837. https://doi.org/10.6026/97320630015832

Arshad Ali, S., Baloch, M., Ahmed, N., Arshad Ali, A., & Iqbal, A. (2020). The outbreak of Coronavirus Disease 2019 (COVID-19)-An emerging global health threat. *Journal of Infection and Public Health*, 13(4), 644–646. https://doi.org/10.1016/j.jiph.2020.02.033

Athir, N., Shi, L., Shah, S. A. A., Zhang, Z., Cheng, J., Liu, J., & Zhang, J. (2019). Molecular dynamics simulation of thermo-mechanical behaviour of elastomer cross-linked via multifunctional zwitterions. *Physical Chemistry Chemical Physics*, 21(38), 21615–21625. https://doi.org/10.1039/C9CP03221E

Boldog, P., Tekeli, T., Vizi, Z., Denes, A., Bartha, F. A., & Rost, G. (2020). Risk assessment of novel coronavirus COVID-19 outbreaks outside China. *Journal of Clinical Medicine*, 9(2), 571. https://doi.org/10.3390/jcm9020571

Burley, S. K., Berman, H. M., Christie, C., Duarte, J. M., Feng, Z. K., Westbrook, J., Young, J., & Zardecki, C. (2018). RCSB Protein Data Bank: Sustaining a living digital data resource that enables breakthroughs in scientific research and biomedical education. *Protein Science*, 27(1), 316–330. https://doi.org/10.1002/pro.3331

Chandra, A., Goyal, N., Qamar, I., & Singh, N. (2020). Identification of hot spot residues on serine-arginine protein kinase-1 by molecular dynamics simulation studies. *Journal of Biomolecular Structure and Dynamics*, 4, 1–9. https://doi.org/10.1080/07391102.2020.1734487

Chaudhari, H. K., & Pahelkar, A. (2019). 3D QSAR, docking, molecular dynamics simulations and MM-GBSA studies of extended side chain of the antitubercular drug (6S) 2-nitro-6- {[4-(trifluoromethoxy) benzyl] oxy}-6,7-dihydro-5H-imidazo[2,1-b] [1,3] oxazine. *Infectiuos Disorders Drug Targets*, 19(2), 145–166. https://doi.org/10.2174/1871526518666181015145545

Chinnasamy, S., Selvaraj, G., Kaushik, A. C., Kaliamurthi, S., Chandrabose, S., Singh, S. K., Thirugnanasambandam, R., Gu, K., & Wei, D. Q. (2019). Molecular docking and molecular dynamics simulation studies to identify potent AURKA inhibitors: Assessing the performance of density functional theory, MM-GBSA and mass action kinetics calculations. *Journal of Biomolecular Structure and Dynamics*, 1–16. https://doi.org/10.1080/07391102.2019.1674695

Chtita, S., Ghamali, M., Ousaa, A., Aouidate, A., Belhassan, A., Taourati, A. I., Masand, V. H., Bouachrine, M., & Lakhlifi, T. (2019). QSAR study of anti-Human African Trypanosomiasis activity for 2-phenylimidazopyridines derivatives using DFT and Lipinski's descriptors. *Heliyon*, 5(3), e01304. https://doi.org/10.1016/j.heliyon.2019.e01304

Çınaroğlu, S. S., & Timuçin, E. (2019). Comprehensive evaluation of the MM-GBSA method on bromodomain-inhibitor sets. *Briefings in Bioinformatics*, 1–14. https://doi.org/10.1093/bib/bbz143

Daoui, S., Faizi, M. S. H., Kalai, F. E., Saddik, R., Dege, N., Karrouchi, K., & Benchat, N. (2019). Crystal structure and the DFT and MEP study of 4-benzyl-2-[2-(4-fluoro-phen-yl)-2-oxoeth-yl]-6-phenyl-pyridazin-3(2H)-one. *Acta Crystallographica Section E Crystallographic Communications*, 75(7), 1030–1034. https://doi.org/10.1107/S2056989019008557

David, A. C., Thomas, E. C., III, Tom, D., Holger, G., Ray, L., Kenneth, M. M., Jr., Alexey, O., Carlos, S., Bing, W., & Robert, J. W. (2005). The Amber Biomolecular Simulation Programs. *Journal of Computational Chemistry*, 26(16), 1668–1688. https://doi.org/10.1002/jcc.20290

De Salazar, P. M., Niehus, R., Taylor, A., Buckee, C. O., & Lipsitch, M. (2020). Identifying locations with possible undetected imported severe acute respiratory syndrome coronavirus 2 cases by using importation predictions. *Emerging Infectious Disease*, 26(7). https://doi.org/10.3201/eid2607.200250

Do, P. C., Lee, E. H., & Le, L. (2018). Steered molecular dynamics simulation in rational drug design. *Journal of Chemical Information and Modeling*, 58(8), 1473–1482. https://doi.org/10.1021/acs.jcim.8b00261

Du, J., Sun, H., Xi, L., Li, J., Yang, Y., Liu, H., & Yao, X. (2011). Molecular modeling study of checkpoint kinase 1 inhibitors by multiple docking strategies and prime/MM-GBSA calculation. *Journal of Computational Chemistry*, 32(13), 2800–2809. https://doi.org/10.1002/jcc.21859

Duan, L., & Zhu, G. (2020). Psychological interventions for people affected by the COVID-19 epidemic. *Lancet Psychiatry*, 7, 300–302. https://doi.org/10.1016/S2215-0366(20)30073-0

Gao, Y., Wang, H., Wang, J., & Cheng, M. (2019). In silico studies on p21-activated kinase 4 inhibitors: Comprehensive application of 3D-QSAR analysis, molecular docking, molecular dynamics simulations, and MM-GBSA calculation. *Journal of Biomolecular Structure and Dynamics*, 1–26. https://doi.org/10.1080/07391102.2019.1673823

Goodsell, D. S., Zardecki, C., Di Costanzo, L., Duarte, J. M., Hudson, B. P., Persikova, I., Segura, J., Shao, C., Voigt, M., Westbrook, J. D., Young, J. Y., & Burley, S. K. (2020). RCSB Protein Data Bank: Enabling biomedical research and drug discovery. *Protein Science*, 29(1), 52–65. https://doi.org/10.1002/pro.3730

Gupta, A., Gandhimathi, A., Sharma, P., & Jayaram, B. (2007). ParDOCK: An all atom energy based Monte Carlo docking protocol for protein-ligand complexes. *Protein and Peptide Letters*, 14(7), 632–646. https://doi.org/10.2174/092986607781483831

Hayes, J. M., Skamnaki, V. T., Archontis, G., Lamprakis, C., Sarrou, J., Bischler, N., Skaltsounis, A. L., Zographos, S. E., & Oikonomakos, N. G. (2011). Kinetics, in silico docking, molecular dynamics, and MM-GBSA binding studies on prototype indirubins, KT5720, and staurosporine as phosphorylase kinase ATP-binding site inhibitors: The role of water

molecules examined. *Proteins: Structure, Function, and Bioinformatics*, *79*(3), 703–719. https://doi.org/10.1002/prot.22890

Hsu, K. C., Chen, Y. F., Lin, S. R., & Yang, J. M. (2011). iGEMDOCK: A graphical environment of enhancing GEMDOCK using pharmacological interactions and post-screening analysis. *BMC Bioinformatics*, *12*(Suppl 1), S33. https://doi.org/10.1186/1471-2105-12-S1-S33

Joshi, T., Joshi, T., Sharma, P., Chandra, S., & Pande, V. (2020). Molecular docking and molecular dynamics simulation approach to screen natural compounds for inhibition of Xanthomonas oryzae pv. Oryzae by targeting peptide deformylase. *Journal of Biomolecular Structure and Dynamics*, 1–18. https://doi.org/10.1080/07391102.2020.1719200

Kalirajan, R., Pandiselvi, A., Gowramma, B., & Balachandran, P. (2019). In-silico design, ADMET screening, MM-GBSA binding free energy of some novel isoxazole substituted 9-anilinoacridines as HER2 inhibitors targeting breast cancer. *Current Drug Research Reviews*, *11*(2), 118–128. https://doi.org/10.2174/2589977511666190912154817

Kumar, D., Kumari, K., Jayaraj, A., & Singh, P. (2019). Development of a theoretical model for the inhibition of nsP3 protease of Chikungunya virus using pyranooxazoles. *Journal of Biomolecular Structure and Dynamics*, 1–17. https://doi.org/10.1080/07391102.2019.1650830

Kumar, D., Singh, P., Jayaraj, A., Kumar, V., Kumari, K., & Patel, R. (2019). A theoretical model to study the interaction of erythro-noscapines with nsP3 protease of chikungunya virus. *ChemistrySelect*, *4*(17), 4892–4898. https://doi.org/10.1002/slct.201803360

Pant, P., Afshan Shaikh, S., & Jayaram, B. (2017). Design and characterization of symmetric nucleic acids via molecular dynamics simulations. *Biopolymers*, *107*(4), e23002. https://doi.org/10.1002/bip.23002

Pereira, G. R. C., Da Silva, A. N. R., Do Nascimento, S. S., & De Mesquita, J. F. (2019). In silico analysis and molecular dynamics simulation of human superoxide dismutase 3 (SOD3) genetic variants. *Journal of Cellular Biochemistry*, *120*(3), 3583–3598. https://doi.org/10.1002/jcb.27636

Roe, D. R., & Cheatham, T. E. (2013). PTRAJ and CPPTRAJ: Software for processing and analysis of molecular dynamics trajectory data. *Journal of Chemical Theory and Computation*, *9*(7), 3084–3095. https://doi.org/10.1021/ct400341p

Roe, D. R., & Cheatham, T. E. (2018). Parallelization of CPPTRAJ enables large scale analysis of molecular dynamics trajectory data. *Journal of Computational Chemistry*, *39*(25), 2110–2117. https://doi.org/10.1002/jcc.25382

Scott, A. H., & Ron, O. D. (2018). Molecular dynamics simulation for all. *Neuron*, *99*(6), 1129-1143. https://doi.org/10.1016/j.neuron.2018.08.011

Singh, P., Kumar, D., Vishvakarma, V. K., Yadav, P., Jayaraj, A., & Kumari, K. (2019). Computational approach to study the synthesis of noscapine and potential of stereoisomers against nsP3 protease of CHIKV. *Heliyon*, *5*(12), e02795. https://doi.org/10.1016/j.heliyon.2019.e02795

Skjevik, A. A., Madej, B. D., Dickson, C. J., Teigen, K., Walker, R. C., & Gould, I. R. (2015). All-atom lipid bilayer self-assembly with the AMBER and CHARMM lipid force fields. *Chemical Communications*, *51*(21), 4402–4405. https://doi.org/10.1039/C4CC09584G

Vora, J., Athar, M., Sinha, S., Jha, P. C., & Shrivastava, N. (2020). Binding insight of anti-HIV phytocompounds with prime targets of HIV: A molecular dynamics simulation analysis. *Current HIV Research*, *18*(2), 132–141. https://doi.org/10.2174/1570162X18666200129112509

Wang, X., Hong, Y., Wang, M., Xin, G., Yue, Y., & Zhang, J. (2019). Mechanical properties of molybdenum diselenide revealed by molecular dynamics simulation and support vector machine. *Physical Chemistry Chemical Physics*, *21*(18), 9159–9167. https://doi.org/10.1039/C8CP07881E

Yuan, S., Chan, H. C. S., & Hu, Z. (2017). Implementing WebGL and HTML5 in macromolecular visualization and modern computer-aided drug design. *Trends in Biotechnology*, *35*(6), 559–571. https://doi.org/10.1016/j.tibtech.2017.03.009

Zhao, J., Xu, X., Li, P., Li, X., Chen, D., Qiao, X., Du, J., Qian, G., & Fan, X. (2019). Structural origins of RF3/NaRF4 nanocrystal precipitation from phase-separated SiO2-Al2O3-RF3-NaF Glasses: A molecular dynamics simulation study. *The Journal of Physical Chemistry B*, *123*(13), 3024–3032. https://doi.org/10.1021/acs.jpcb.9b01674